ISSN (Print) 1226-1750
ISSN (Online) 2233-6656
Journal of Magnetics 25(1), 29-35 (2020) https://doi.org/10.4283/JMAG.2020.25.1.029

Comparison of Hot-deformation Behavior and Magnetic Properties between Nd-Fe-B HDDR and MQU-F Powder

Jae-Gyeong Yoo[1,2], Hee-Ryoung Cha[1], Dong-Hwan Kim[3], Yang-Do Kim[2]*, and Jung-Goo Lee[1]*

[1]Powder & Ceramics Division, Korea Institute of Materials Science, 797 Changwon-daero, Changwon 51508, Republic of Korea
[2]Department of Materials Science and Engineering, Pusan National University, 2, Busandaehak-ro 63beon-gil, Geumjeong-gu, Busan 46241, Republic of Korea
[3]Research Center of SG Tech., Star Group Ind. Co., Ltd., 49, Dalseo-daero 85-gil, Dalseo-gu, Daegu, Republic of Korea

(Received 30 August 2019, Received in final form 16 February 2020, Accepted 20 February 2020)

Hot-deformation behavior of Nd-Fe-B HDDR powder was investigated in order to understand the difference in texturing mechanism of HDDR and MQU-F powder during hot-deformation. The composition of the HDDR powder was the same as that of MQU-F powder. However, the grain size of HDDR powder (~300 nm) was eight times larger than that of MQU-F powder (~40 nm). After being subjected to hot-pressing at 700 °C under 200 MPa in a vacuum, the grains of the magnets made from HDDR powder and MQU-F powder have globular and platelet shapes, respectively. The remanence was 12.2 kG after die-upsetting process at the strain of 0.5. And it increased up to 13 kG at the strain of 1.4 although the grains still maintained globular-like shapes. The remanence of 13 kG was almost the same as that obtained the magnet from MQU-F powder at the same deformation condition. These results indicate that the hot-deformation behavior is quite different between HDDR and MQU-F powder.

Keywords : Nd-Fe-B, HDDR, Hot-deformation

1. Introduction

Nd-Fe-B permanent magnets have been indispensable for traction motors of electric/hybrid vehicles and generators of wind turbines due to their excellent magnetic properties, especially the highest maximum energy product $(BH)_{max}$ [1, 2]. For these applications, however, quite high coercivity must be achieved at room temperature due to the high operating temperature. Compared to commercial sintered magnets with micrometer-sized grains, hot-deformed magnets have the potentials to obtain high coercivity and improve the thermal stability without using heavy rare-earth (HRE) elements due to their ultrafine grains with single domain size [3, 4]. Nanocrystalline anisotropic Nd-Fe-B magnet fabricated by hot-deformation process with isotropic melt-spun ribbons was first reported by Lee *et al.* [5]. Generally, the hot-deformation process consists of two steps, namely, hot-pressing and die-upsetting. First, Nd-Fe-B nanocrystalline flakes or powders are hot-pressed to form high density isotropic compact. Second, the $Nd_2Fe_{14}B$ grains are aligned along their easy magnetization c-axis parallel to the compression direction during die-upsetting [6-8].

The mechanism of texture formation during hot-deformation process has been extensively studied for melt-spun powders. It has been reported that grains grow along the [010] and [100] axis into platelet shape and align along the [001] axis parallel to the pressing direction by the interface-controlled solution-precipitation-creep process and grain boundary sliding during hot-deformation [8, 9]. On the other hands, the grains of hot-deformed magnet made from melt-spun powder can be easily grown at temperatures higher than 700 °C due to their ultrafine grain size, decreasing coercivity of magnet. However, the hot-deformed magnet made from hydrogenation–disproportionation–desorption–recombination (HDDR) powder has relatively coarser-grains compared to that of melt-spun powder. Therefore, it could be subjected to heat-treatment at temperatures higher than 700 °C without significant grain growth. This means that the limitation of the post-heat treatment for the coercivity enhancement of

*Co-Corresponding author: Tel: +82-55-280-3606
Fax: +82-55-280-6788, e-mail: jglee36@kims.re.kr
Tel: +82-51-510-2478, Fax: +82-51-512-0528
e-mail: yangdo@pusan.ac.kr

the hot-deformed magnet could be removed. Thus, the HDDR powder could be a good candidate for hot-deformation process to make high-performance magnets.

There are a few reports on hot-deformation using HDDR powder, which examined the relationship between magnetic properties and processing condition such as temperature, strain and strain rate [10-13]. Liesert *et al.* studied the influence of Nd content and the grain size of HDDR powders on the die-upsetting [14]. However, systematic studies on the hot-deformation behavior of HDDR powders during hot-deformation are quite limited.

Especially, the grain texturing mechanism of HDDR powder during hot-deformation is rarely reported. Therefore, in this study, hot-deformation behavior and magnetic properties between Nd-Fe-B HDDR and MQU-F powder was compared to get an understanding of texturing mechanism of HDDR powder during hot-deformation.

2. Experimental

The $Nd_{13.6}Fe_{73.6}Co_{6.6}Ga_{0.6}B_{5.6}$ mold-cast alloy with the same composition as the commercial melt-spun powder (MQU-F) was first subjected to homogenization heat treatment at 1000 °C for 27 h under Ar atmosphere in the tube furnace. It was then transferred to a glove box which was directly connected to the furnace, and crushed into powders in the size range from 200 to 300 μm. After being transferred to the furnace again, the powders were subjected to HDDR treatment to obtain ultra-fine grained isotropic powders. The HDDR treatment was carried out as follows: First, the powders were heated up to 840 °C under H_2 gas atmosphere with a pressure of 1.1 atm. When the temperature reached up to 840 °C, H_2 gas was maintained at a pressure of 1.1 atm for 60 min to induce an HD (hydrogenation-disproportionation) reaction. In the DR (desorption-recombination) stage, the furnace was evacuated with a rotary pump and maintained for 20 min. Finally, the powders were quenched down to room temperature using Ar gas. After HDDR treatment, the powders were consolidated into Nd–Fe–B isotropic magnet by hot-pressing at 700 °C under 200 MPa in a vacuum. The cylindrical compacts with 7 mm in diameter and 6 mm in height were then subjected to die-upsetting at 700 °C with strain rates of 0.01 s^{-1} and 0.001 s^{-1}. A deformation degree of ε = 0.5-1.4 [$\varepsilon = \ln(h_0/h)$; h_0: starting height of the sample; h: height after deformation] was realized, which corresponds to 40%-75% height reduction. The microstructure after hot-deformation was observed by the field emission scanning electron microscope (FESEM). For the FESEM observation, the samples were polished and subsequently etched with a H_2SO_4 aqueous solution of 0.1 M for 30 s at room temperature. The magnetic properties of samples were measured using a vibrating sample magnetometer (VSM) with a rectangular parallelepiped (3×3×1 mm^3) which was cut from the center area of hot-deformed magnets and magnetized with 6T pulsing magnetic field. Additionally, the microstructure and magnetic properties of hot-deformed magnet using HDDR powder was compared with those using MQU-F powder.

3. Results and Discussion

Figure 1 shows demagnetization curves of initial powders, hot-pressed and die-upset magnets made from HDDR and MQU-F powder, respectively. The remanence of the initial HDDR and MQU-F powder was about 7.5 and 8 kG, respectively, which means that the grains of both powders

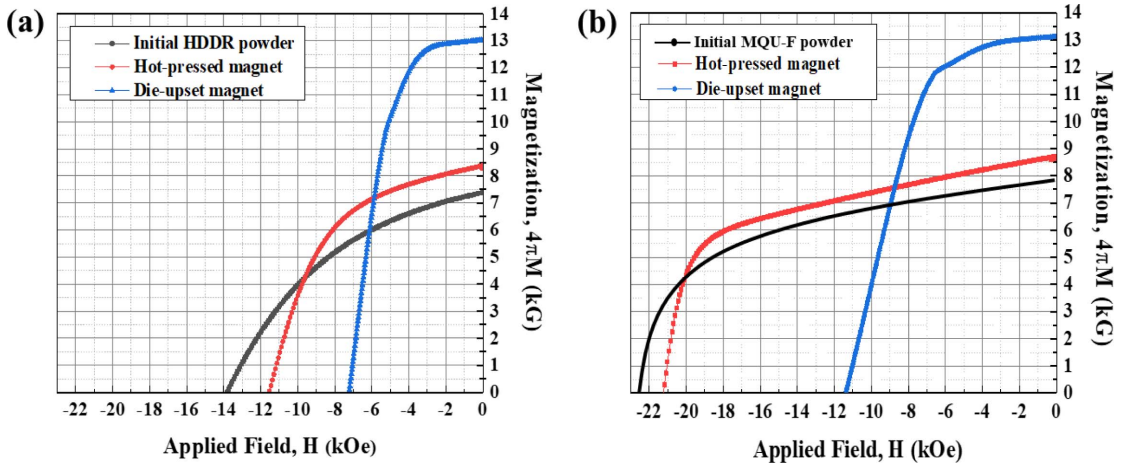

Fig. 1. (Color online) Demagnetization curves of initial powders, hot-pressed and die-upset magnet made from (a) HDDR and (b) MQU-F powder [15] with a strain of 1.4 and a strain rate of 0.01.

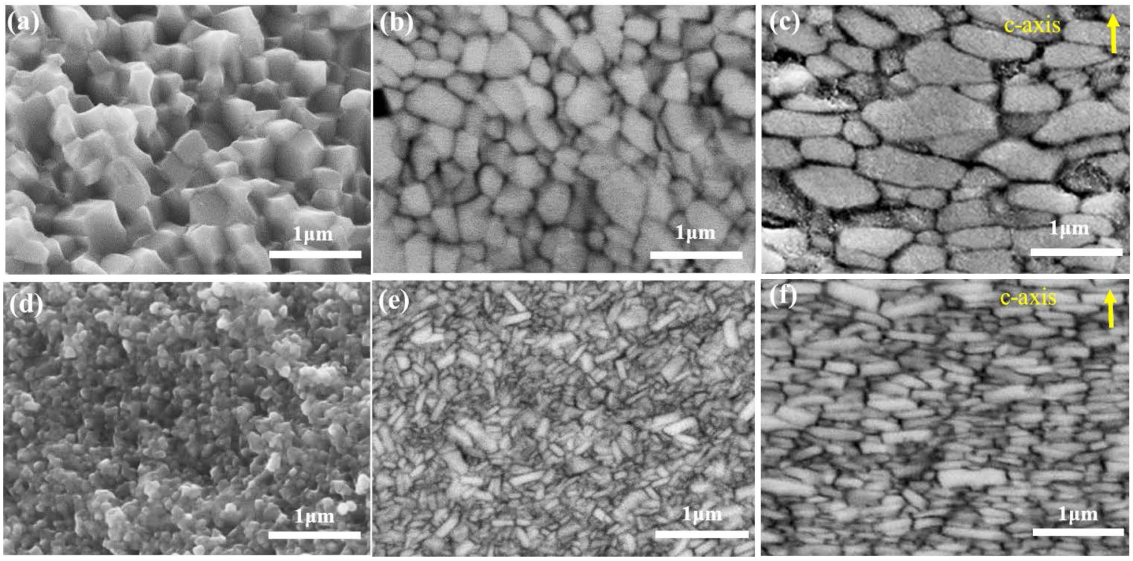

Fig. 2. (Color online) SEM image of fracture surface of initial (a) HDDR and (d) MQU-F powder. SEM image of polished-etched surface of the hot-pressed magnets made from (b) HDDR and (e) MQU-F powder [15] and the die-upset magnet made from (c) HDDR and (f) MQU-F powder [15].

are randomly oriented. The coercivity of the initial HDDR and MQU-F powders were approximately 14 and 22 kOe, respectively. On the other hand, the remanence was largely increased up to 13 kG after hot-deformation with a strain of 1.4 regardless of the kind of initial powder. This is because the magnetic easy axis of the grains was aligned parallel to the pressing direction [8, 9].

Figure 2 shows typical microstructures of initial powders, hot-pressed and die-upset magnets made from HDDR and MQU-F powders, respectively. The average grain size of the HDDR powder was 300 nm which is close to the single domain size of $Nd_2Fe_{14}B$ phase and eight times larger than that of MQU-F powder as shown in Fig. 2(a) and (d). With regard to the MQU-F powder, randomly oriented platelet-shaped grains were observed after hot-pressing due to grain growth along a-axis. The short axis of grains corresponding to the c-axis were aligned parallel to the pressing direction during die-upsetting as shown in Fig. 2(e) and (f), which is well consistent with those expected from the reported texturing mechanism of melt-spun powder [7, 8]. For the HDDR powder, however, there was a significant difference in microstructural evolution during hot-deformation. There was no remarkable grain growth, especially along the a-axis in the hot-pressed magnet made from HDDR powder as shown in Fig. 2(a) and (b).

After die-upsetting, the shape of grains changed from spherical to platelet-like, and the grains were aligned with their c-axis parallel to the pressing direction. However, the aspect ratio of grains (the ratio of length to width of grain) is quite different from that of die-upset magnet using MQU-F powder as shown in Fig. 2(c) and (f). In Table 1, the grain aspect ratio of initial powders, hot-pressed and die-upset magnets made from HDDR and MQU-F powders were summarized. For the HDDR powder, most of grain aspect ratio after die-upsetting ranged from 1.5 to 3, which is much smaller than that of the MQU-F powder. Therefore, it can be concluded that the grain size of the initial powder strongly affects the grain shape, especially the grain aspect ratio of the hot-deformed magnets because we employed two kinds of initial powders having the same composition but different grain sizes. On the other hand, high aspect ratio grains after hot-pressing are favorable for grain rotation by grain boundary sliding during die-upsetting, which results in high degree of grain alignment, increasing the remanence of magnet.

For the HDDR powder, however, the aspect ratio of grains after hot-pressing is almost 1. This indicates that grain rotation by grain boundary sliding is much more difficult to occur during die-upsetting compared to hot-

Table 1. Grain aspect ratio of initial powder, hot-pressed and die-upset magnet made from HDDR and MQU-F powders [15].

	Grain aspect ratio	
	HDDR	MQU-F
Initial powder	~1	~1
Hot-pressed magnet	1~1.3	2.5~5
Die-upset magnet	1.5~3	3~6

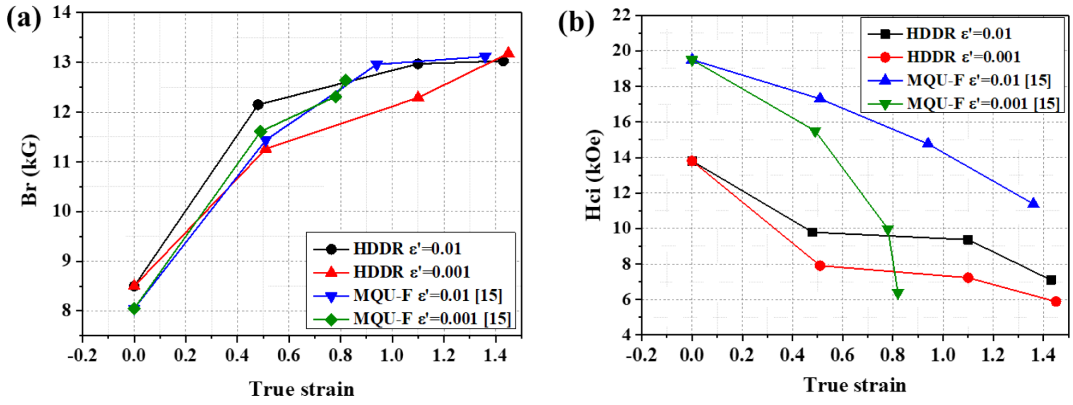

Fig. 3. (Color online) Dependence of (a) remanence and (b) coercivity of die-upset magnets made from HDDR and MQU-F powders [15] at two different strain rates on the true strain.

pressed magnet from the MQU-F powder. However, it should be noted that the remanence is almost the same regardless of the type of initial powder, which means that a different mechanism for c-axis alignment parallel to the pressing direction would operate during die-upsetting of the HDDR powder.

To compare hot-deformation behavior between HDDR and MQU-F powders, we investigated the effect of strains and strain rates on the magnetic properties, as well as microstructure evolution during die-upsetting. Figure 3(a) shows the change of remanence during die-upsetting using HDDR and MQU-F [15] powders with different strain rates which are $\dot{\varepsilon} = 0.01\ s^{-1}$ (hereafter called fast strain rate) and $\dot{\varepsilon} = 0.001\ s^{-1}$ (hereafter called slow strain rate). The remanence of die-upset magnets was gradually increased with increasing strain because of improved grain alignment. In the strain range of < 0.5, the degree of remanence enhancement was stronger at the fast strain rate than at the slow strain rate in the magnet made from HDDR powder, while it was stronger at the slow strain rate than at the fast strain rate in that from MQU-F powder. The remanence of magnet made at the fast strain rate using HDDR powder was high as 12.2 kG in spite of a low strain of 0.47. However, this tendency was changed with increasing strain. In the stain range of > 0.5, the degree of remanence enhancement was stronger at the slow strain rate than at the fast strain rate in the magnet made from HDDR powder. Here, the remanence reached 13 kG, which is almost the same as that of MQU-F powder at strain of 1.4 and the fast strain rate. For the magnet made from MQU-F powder, however, it could not be deformed more than $\varepsilon = 0.9$ at the slow strain rate, which shows a remanence of 12.6 kG.

On the other hand, the coercivity gradually decreased with increasing strain regardless of the strain rates, although slower strain rates induced a larger decrease of coercivity, as shown Fig. 3(b). It is noteworthy to mention that the dependence of coercivity decline on the strain rate during die-upsetting is quite different between hot-pressed magnets from HDDR and MQU-F powders. The MQU-F powder showed a much stronger dependence of coercivity decline on the strain rate compared to HDDR powder during die-upsetting.

Figure 4 shows the microstructure evolution of hot-pressed magnets from HDDR and MQU-F powders during die-upsetting at different strains and strain rates. Fig. 4(a) and (b) show the microstructure evolution of hot-pressed magnet from HDDR powder with increasing strain at fast and slow strain rates, respectively. The grains of die-upset magnet at the fast strain rate with HDDR powder were grown from 300 nm to approximately 1-2 μm, which had an aspect ratio of 1.5-3. Additionally, at the slow strain rate, grains were grown up to ~3 μm after die-upsetting at the slow strain rate and a strain of 1.4. This is because that the slow strain rate would facilitate grain growth due to the longer time of exposure to heat compared to the fast strain rate.

Figure 4(c) and (d) show the microstructural evolution of the hot-pressed magnet from MQU-F powder with increasing strain at fast and slow strain rates, respectively [15]. For the MQU-F powder, the randomly oriented platelet-shaped grains were gradually aligned along the [001] axis, parallel to the pressing direction with increasing strain during die-upsetting. The grain sizes of die-upset magnet at both the fast and slow strain rate with MQU-F powder were almost the same as those of hot-pressed magnet with lengths of 300-500 and widths of 50-100 nm, which had an aspect ratio of 3-6. On the other hand, the die-upset magnet with a strain of 0.9 at the slow strain rate shows quite indistinct grain boundaries [marked dotted yellow line in Fig. 4(d)]. In our previous result, it was confirmed that prolonged deformation time with slow

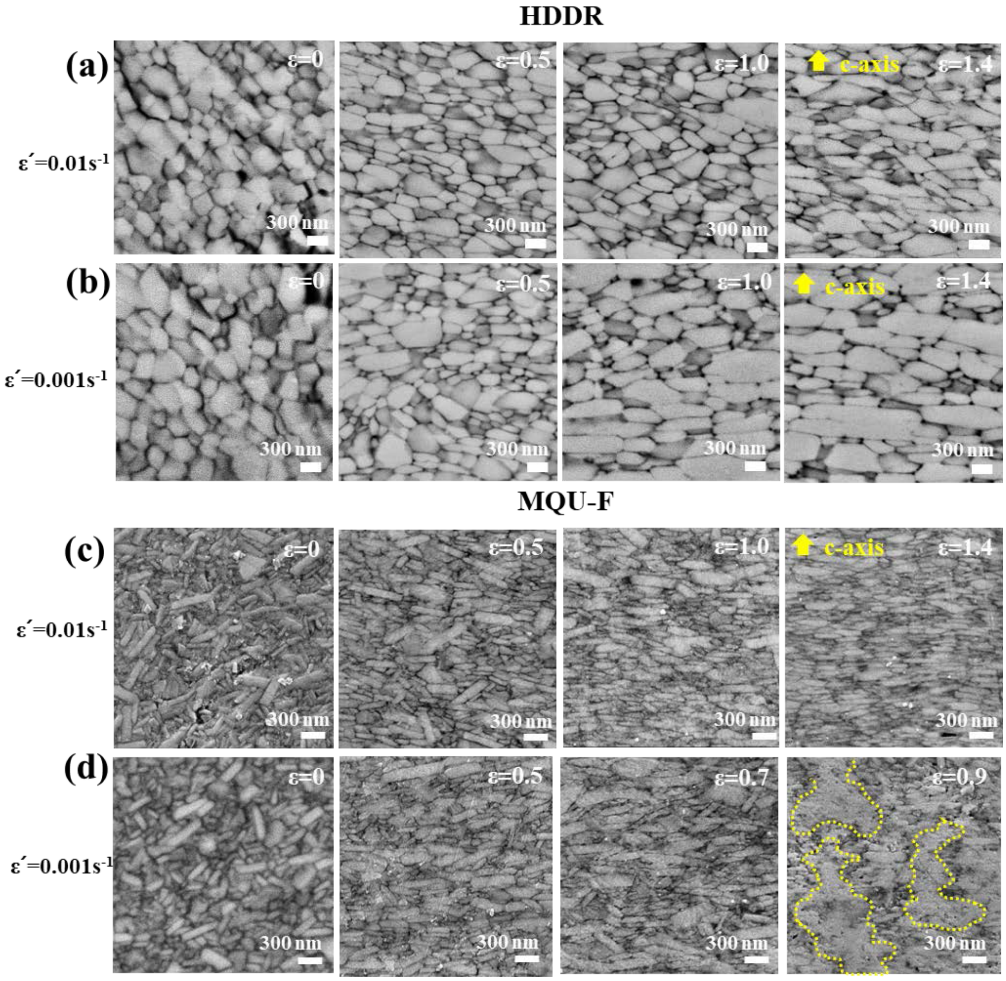

Fig. 4. (Color online) SEM images of polished-etched surface of die-upset magnets made from [(a), (b)] HDDR and [(c), (d)] MQU-F powder [15] at the strain rate of [(a), (c)] 0.01 s^{-1} and [(b), (d)] 0.001 s^{-1}, with increasing strain.

strain rates induced the squeeze-out of Nd-rich phase at the grain boundary [15]. This is because after the course of grains' alignment, Nd-rich phase at grain boundaries perpendicular to the pressing direction could receive quite a large amount of pressure, and thus easily squeezed out. Then, the Nd-rich grain boundary phase is gradually thinned, and finally disappears as shown Fig. 4(d). For the HDDR powder, however, there was no squeeze-out of Nd-rich grain boundary phase during die-upsetting at the slow strain rate as shown in Fig. 4(b). Therefore, it could be explained that the rapid reduction in coercivity of die-upset magnet at the slow strain rate using MQU-F powder (Fig. 3(b)) was due to the formation of a non-uniform and discontinuous grain boundary caused by squeeze-out of Nd-rich phase during die-upsetting, which could enhance magnetic coupling between neighbor grains, decreasing the coercivity. This is also reported that longer deformation process at a lower strain rate lead to not only lower coercivity due to grain coarsening but also lower remanence due to poor grain alignment [16].

Figure 5 shows true stress-strain curves of hot-pressed magnets made from HDDR and MQU-F powders during die-upsetting at two different strain rates. It should be noted that the dependence of the stress-strain curve on the strain rate was significantly different between HDDR and MQU-F. In Figure 5, the true stresses of magnets were gradually increased with increasing strain. However, the strain rate dependence on the stress of the magnet from MQU-F powder was much stronger than that of the magnet from HDDR powder. In the magnet from MQU-F powder, it received lower stress at a slow stain rate below approximately $\varepsilon = 0.5$. However, the stress increased much faster than that at the fast strain rate. Especially, at slow strain rate, the magnet could not be deformed more than $\varepsilon = 0.9$ despite a considerable stress higher than 800 MPa [15]. In the magnet from HDDR powder, the tendency of strain-rate dependence is similar to that from MQU-F powder. However, the strain-stress curves in Fig. 5(a)

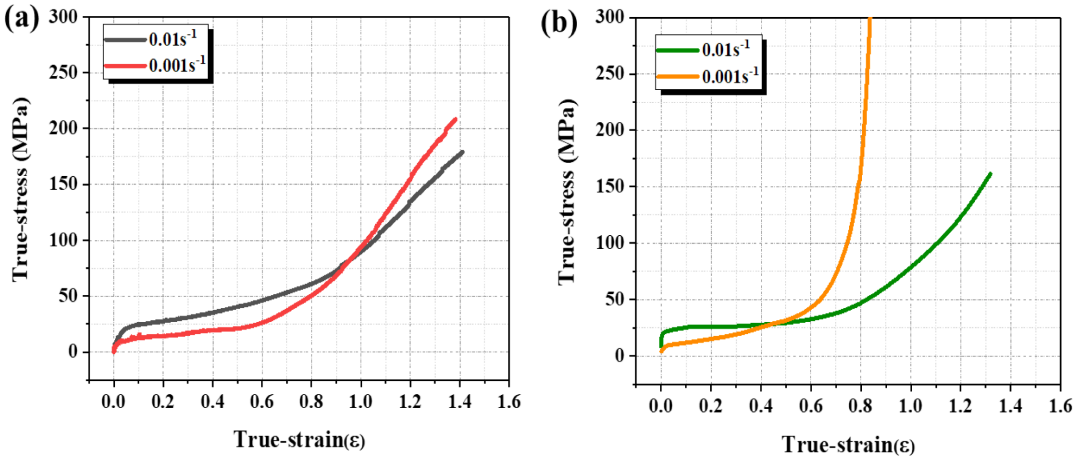

Fig. 5. (Color online) True stress-strain curves of hot-pressed magnets made from (a) HDDR and (b) MQU-F powders [15] during die-upsetting at two different strain rates.

show a much weaker degree of strain-rate dependence as compared to those in Fig. 5(b). The magnet from HDDR powder could be deformed up to $\varepsilon = 1.4$ at both the fast and slow strain rate. For the magnet from MQU-F powder, a longer processing time at the slow strain rate, which is the cause of the squeeze-out of Nd-rich phase from the grain boundaries limited deformation degree. This result is consistent with the result of the microstructure in Fig. 4(d). On the other hand, For the magnet from HDDR powder, the specimen shows a clear and continuous Nd-rich phase at grain boundaries in both the fast and slow strain rate in Fig. 4(a) and (b) after die-upsetting. It could be expected that the magnet from HDDR powder was deformed up to $\varepsilon = 1.4$ at both the fast and slow strain rates due to the uniform and continuous liquid Nd-rich phase during die-upsetting. Most studies suggest that the deformation behavior of Nd–Fe–B alloys during die-upsetting is associated with a solution–precipitation creep process and grain boundary sliding [6-8]. However, Luo *et al.* measured the Young's modulus parallel or perpendicular to the c-axis for the $Nd_2Fe_{14}B$ phase and suggested that the crystal rotation associated with the slip deformation on the (0 0 1) plane led to the texture formation in die-upset magnet [9, 17]. It is also noted that the elastic constant parallel to the c-axis was lower than that parallel to the a-axis [18, 19]. These studies suggest that the elastic anisotropy of the $Nd_2Fe_{14}B$ phase leads to texture formation, which can obtain anisotropic hot-deformed magnet. Based on this study, the $Nd_2Fe_{14}B$ grain of HDDR powder compared to the grain of MQU-F powder is expected to be textured by elastic anisotropy, which facilitates c-axis rotation parallel to the pressing direction during die-upsetting. This is because the $Nd_2Fe_{14}B$ phase with its c-axis parallel to the pressing direction has lower energy compared to the grain with its c-axis perpendicular to the pressing direction. However, further study is needed to clarify the exact texturing mechanism of HDDR powder during die-upsetting.

4. Conclusions

The comparison of the hot-deformation behavior and magnetic properties between Nd-Fe-B HDDR and MQU-F powder during hot-deformation has been studied. The grain size of the obtained HDDR powder (~300 nm) was eight times larger than that of the MQU-F powder (~40 nm). After hot-pressing, the grain size and shape of the magnet made from HDDR powder were almost the same as that of initial powders, whereas, that of the magnet made from MQU-F reveals a platelet-shape with grain growth. After die-upsetting, although the grain shape of the magnet made from HDDR powder was still close to a globular shape, the remanence increased up to 12.2 kG due to the improved grain alignment with a strain of 0.47 and the fast strain rate. The remanence reached 13 kG upon with increasing the strain to 1.4, which is almost the same as that of MQU-F powder. This result is difficult to explain with well-known texturing mechanisms such as grain shape change and grain boundary sliding for melt-spun powder during hot-deformation because the grain shape did not change significantly to platelet-like during hot-deformation in the strain range of < 0.5.

On the other hand, the coercivity decline of die-upset magnet made from MQU-F powder on the strain was much stronger than that of HDDR powder due to the formation of a non-uniform and discontinuous grain boundary caused by squeeze-out of Nd-rich phase during die-upsetting, which could enhance magnetic coupling

between neighbor grains, decreasing the coercivity.

Acknowledgements

This work was supported by the Ministry of Trade, Industry and Energy, South Korea, through the Industrial Strategic Technology Development Program under Grant 20000401, 10080382.

References

[1] S. Sugimoto, J. Phys. D **44**, 064001 (2011).
[2] K. Hono and H. Sepehri-Amin, Scr. Mater. **67**, 530 (2012).
[3] O. Gutfleisch, M. A. Willard, E. Brück, C. H. Chen, S. Sankar, and J. P. Liu, Adv. Mater. **23**, 821 (2011).
[4] J. Liu, H. Sepehri-Amin, T. Ohkubo, K. Hioki, A. Hattori, T. Schrefl, and K. Hono, Acta. Materialia. **82**, 336 (2015).
[5] R. Lee, Appl. Phys. Lett. **46**, 790 (1985).
[6] D. Brown, Z. Wu, F. He, D. Miller, and J. Herchenroeder, J. Phys.: Condens. Matter **26**, 064202 (2014).
[7] W. Grünberger, D. Hinz, A. Kirchner, K. Müller, and L. Schultz, J. Alloys Compd. **257**, 293 (1997).
[8] T. Mouri, M. Kumano, H. Yasuda, T. Nagase, R. Kato, Y. Nakazawa, and H. Shimizu, Scr. Mater. **78**, 37 (2014).
[9] H. Yasuda, M. Kumano, T. Nagase, R. Kato, and H. Shimizu, Scr. Mater. **65**, 743 (2011).
[10] P. McGuiness, C. Short, A. Wilson, and I. Harris, J. Alloys Compd. **184**, 243 (1992).
[11] O. Gutfleisch, A. Kirchner, W. Grünberger, D. Hinz, H. Nagel, P. Thompson, J. Chapman, K. Müller, L. Schultz, and I. Harris, J. Phys. D **31**, 807 (1998).
[12] O. Gutfleisch, A. Kirchner, W. Grünberger, D. Hinz, R. Schäfer, L. Schultz, I. Harris, and K. Müller, J. Magn. Magn. Mater. **183**, 359 (1998).
[13] A. Kirchner, W. Grünberger, O. Gutfleisch, V. Neu, K. Müller, and L. Schultz, J. Phys. D **31**, 1660 (1998).
[14] S. Liesert, A. Kirchner, W. Grünberger, A. Handstein, P. De Rango, D. Fruchart, L. Schultz, and K. Müller, J. Alloys Compd. **266**, 260 (1998).
[15] H. Cha, S. Liu, J. Yu, H. Kwon, Y. Kim, and J. Lee, IEEE Trans. Magn. **51**, 2101704 (2015).
[16] R. Zhao, W. Zhang, J. Li, H. Wang, M. Zhu, and W. Li, J. Magn. **16**, 294 (2011).
[17] R. K. Mishra, J. Appl. Phys. **62**, 967 (1987).
[18] L. Li and C. Graham, IEEE Trans. Magn. **28**, 2130 (1992).
[19] R. Chen, Z. Wang, X. Tang, W. Yin, C. Jin, J. Ju, D. Lee, and A. Yan, Chinese Physics B **27**, 117504 (2018).